Published May 15, 1993

The Organization of F-Actin and Microtubules in Growth Cones Exposed to a Brain-derived Collapsing Factor

Jinhong Fan, S. Gary Mansfield,* Tim Redmond,‡ Phillip R. Gordon-Weeks,* and Jonathan A. Raper

Department of Neurosciences, University of Pennsylvania School of Medicine, Philadelphia, Pennsylvania 19104; *Developmental Biology Research Centre, King's College, London; and ‡Department of Biology, University of Pennsylvania, Philadelphia, Pennsylvania 19104

Abstract. In previous work we characterized a brain derived collapsing factor that induces the collapse of dorsal root ganglion growth cones in culture (Raper and Kapfhammer, 1990). To determine how the growth cone cytoskeleton is rearranged during collapse, we have compared the distributions of F-actin and microtubules in normal and partially collapsed growth cones. The relative concentration of F-actin as compared to all proteins can be measured in growth cones by ratioing the intensity of rhodamine-phalloidin staining of F-actin to the intensity of a general protein stain. The relative concentration of F-actin is decreased by about one half in growth cones exposed to collapsing factor for five minutes, a time at which they are just beginning to collapse. During this period the relative concentration of F-actin in the leading edges of growth cones decreases dramatically while the concentration of F-actin in the centers decreases little. These results suggest that collapse is associated with a net loss of F-actin at the leading edge.

The distributions of microtubules in normal and collapsing factor treated growth cones were examined with antibodies to tyrosinated and detyrosinated isoforms of α-tubulin. The tyrosinated form is found in newly polymerized microtubules while the detyrosinated form is not. The relative proximal-distal distributions of these isoforms are not altered during collapse, suggesting that rates of microtubule polymerization and depolymerization are not greatly affected by the presence of collapsing factor. An analysis of the distributions of microtubules before and after collapse suggests that microtubules are rearranged, but their polymerization state is unaffected during collapse. These results are consistent with the hypothesis that the brain derived collapsing factor has little effect on microtubule polymerization or depolymerization. Instead it appears to induce a net loss of F-actin at the leading edge of the growth cone.

NEURONAL growth cones navigate on highly reproducible and cell specific pathways. Their trajectories are controlled by cues in their local environment, and these cues are likely to be either permissive or repulsive in nature. Most of the known permissive molecules are thought to act as adhesion molecules (e.g., Burmeister and Goldberg, 1988; Hammarback et al., 1988) or chemoattractants (e.g., Gundersen and Barrett, 1980; Lumsden and Davies, 1983), but little is known about the mechanisms through which repulsive molecules might function.

We are characterizing a growth cone collapsing activity from chick brain that we believe may act as a repulsive guidance cue. This activity can be recovered from membrane preparations made from both embryonic and adult central nervous system tissues, but not from primary fibroblasts or liver cell membranes. Its effects are rapid, reversible, and independent from the substratum on which the growth cones crawl. The activity is basic, trypsin sensitive, heat labile, binds to several lectins, and has an apparent molecular weight of about 100 kD (Raper and Kapfhammer, 1990; Luo, Y., D. Raible, and J. A. Raper, unpublished data).

Since the brain derived collapsing factor induces a reversible and dramatic alteration in structure, we hypothesized that its effects may be mediated by changes in the organization of the cytoskeleton. Rearrangements of cytoskeletal components, particularly actin and microtubules, are thought to alter cell shape in a wide variety of systems. Actin in particular is thought to play a key role in the process of cell motility (review by Cooper, 1991). Actin is one of the major cytoskeletal components of growth cones. Fibrillar (F)[1] actin extends as a meshwork throughout lamellipodia and is densely bundled in filopodia (Yamada et al., 1970; Spooner and Holladay, 1981; Letourneau and Ressler, 1983; Forscher and Smith, 1988). F-actin is continuously polymerized and depolymerized in motile cells and growth cones. It appears to be preferentially polymerized at their leading edges (Forscher and Smith, 1988; Okabe and Hirokawa, 1991; Symons and Mitchison, 1991), and is then translocated centripetally, or

1. *Abbreviations used in this paper*: BB, blocking buffer, DRG, dorsal root ganglia; F, fibrillar.

Published May 15, 1993

left behind as the leading edge advances (Wang, 1985; Okabe and Hirokawa, 1991; Theriot and Mitchison, 1991).

Cytochalasins, a group of plant alkaloids that inhibit actin polymerization, paralyze normal growth cone motility and inhibit axonal extension (Yamada et al., 1970; Letourneau et al., 1987). Growth cones treated with cytochalasins in vivo or in vitro advance extremely slowly and have abnormal morphologies that lack lamellipodia and filopodia. This suggests that actin polymerization is required for normal motility (Marsh and Letourneau, 1984; Bentley and Toroian-Raymond, 1986). Cytochalasin B treatment of growth cones grown on polylysine coated coverslips can cause an F-actin free zone to form behind the leading edges of lamellipodia (Forscher and Smith, 1988). Removal of the drug causes F-actin to fill in, starting from the leading edge and then moving toward the centers of growth cones. This study further supports the hypothesis that actin is constantly polymerized at the leading edges of growth cones and is then translocated towards their centers. It seems likely that this actin cycling could drive the advancement of motile cells and growth cones (Hill and Kirschner, 1982; Theriot et al., 1992), particularly if the F-actin is linked through cell surface receptors to a substratum that supports growth (Smith, 1988; Egelhoff and Spudich, 1991).

Microtubules are another major cytoskeletal component of growth cones that may have a role in controlling their motility. Microtubules are bundled in axons and splay out within the lamellipodia (e.g., Letourneau and Ressler, 1983; Gordon-Weeks et al., 1989). The distal tips of microtubules often reach the leading edges of lamellipodia and occasionally enter filopodia (Shaw et al., 1981; Spooner and Holladay, 1981; Letourneau and Ressler, 1983; Tanaka and Kirschner, 1991). Growth cones contain a large soluble pool of tubulin (Gordon-Weeks and Lang, 1988; Gordon-Weeks et al., 1989) which can polymerize and depolymerize within the growth cones (Letourneau and Ressler, 1984; Bamburg et al., 1986; Gordon-Weeks, 1987; Gordon-Weeks et al., 1989). Individual microtubules have been observed to rapidly lengthen or shorten in living growth cones, perhaps even invading some regions of a growth cone in seeming preference to others (Tanaka and Kirschner, 1991). It has been proposed that the preferential polymerization or stabilization of microtubules in one region of a growth cone may lead to the growth cone's selective protrusion and advancement in that area (Gordon-Weeks, 1991; Sabry et al., 1991).

Agents that interfere with microtubule assembly affect growth cone motility and block axonal extension in culture. Colchicine and its analogue colcemid bind noncovalently to tubulin dimers, prevent assembly, and thereby create equilibrium conditions favorable for the depolymerization of microtubules (review by Hamel, 1990). Both drugs halt axonal extension (Seeds et al., 1970; Yamada et al., 1970; Daniels, 1971), and their primary effect has been suggested to be on growth cones (Bamburg et al., 1986; Keith, 1990). In contrast to agents that lead to microtubule depolymerization, taxol facilitates polymerization by lowering tubulin's critical concentration for polymerization (Schiff et al., 1979). Axons exposed to micromolar concentration of taxol cease to elongate and their growth cones round-up and become immobilized. Microtubules in these growth cones have a distinctive abnormal organization. They are densely packed, tangled, and looped back upon themselves (Letourneau and Ressler, 1984; Gordon-Weeks et al., 1989; Mansfield and Gordon-Weeks, 1991).

Since drugs that perturb actin and microtubule polymerization are known to interfere with growth cone motility, we have studied the effects of a brain derived collapsing factor on actin and microtubule organization in growth cones. We found no evidence that the state of microtubule organization is significantly altered by the collapsing factor. We did find evidence, however, supporting the hypothesis that the collapsing factor ultimately induces the loss of F-actin, particularly in the leading edges of growth cones. Moreover, our results are consistent with the hypothesis that this loss of F-actin leads to the collapse of growth cone structure.

Materials and Methods

Cell Culture

Tissue culture dishes were prepared by drilling a 1-cm-wide hole in the bottom of 35-mm tissue culture dishes which were then sterilized by UV irradiation. Nitric acid-washed, silanized, and UV-sterilized coverslips (Chang et al., 1987) were sealed onto the bottoms of the dishes with silicon grease. The coverslips were soaked in a solution of 40 μg/ml laminin (GIBCO-BRL, Gaithersburg, MD) in Hank's solution for 30 min at 37°C before the plating of neural explants.

The dorsal root ganglia (DRGs) from embryonic day seven chick embryos were cut into halves or quarters and then plated onto the laminin-coated coverslips. Explants were cultured for 18–28 h in F-12 medium (GIBCO-BRL; 320-1765 PK; supplemented with 200 μg/ml bovine pituitary extract (Tsao et al., 1982) dialyzed overnight against F-12 medium, 14 mM $NaHCO_3$, 2 mM glutamine, 100 U/ml penicillin, 100 μg/ml streptomycin, 6 mg/ml glucose, 5 μg/ml insulin, 5 μg transferrin, 5 ng/ml selenious acid, 100 μM putrescine, 20 nM progesterone, and 20 ng/ml 7 S NGF. Cultures were maintained at 37°C and at 5% CO_2.

Videomicroscopy

Before being moved to the heated stage of a microscope for observation, the culture medium was replaced by a CO_2-independent medium in which 14 mM NaCl and 20 mM Hepes at pH 7.4 were used to replace $NaHCO_3$. 0.5–1.0 ml of mineral oil (Sigma, St. Louis, MO) that had been pre-equilibrated with F-12 was layered on top of the medium to prevent evaporation during the experiment. Cultures were maintained at 37°C in a micro-incubator (OPMI-2, controlled by a TC-102 temperature controller; Medical Sys., Greenvale, NY) mounted on an inverted microscope (Axiovert 10; Carl Zeiss, Oberkochen, Germany). Growth cones were viewed in phase contrast through a 40× or 63× Plan lens (Carl Zeiss). The image was further magnified by a 1.6× Optovar.

Time-lapse recording was performed with a vidicon camera (C2400; Hamamatsu Photonics, Hamamatsu City, Japan). The image from the camera was averaged, contrast enhanced, and had a background image subtracted by an image processor (DVS-3000; Hamamatsu Photonics). The resulting image was recorded with an optical disc recorder (TQ-2028F; Panasonic) at regular time intervals (from 1 frame/10 sec to 1 frame/60 s).

Double Labeling for Tubulin Isoforms and F-actin

Cultures treated with collapsing factor for varying lengths of time were fixed in 3% paraformaldehyde, 0.2% glutaraldehyde, 20 mM EGTA, 0.065% Triton X-100 in PBS, pH 7.3, for 10 min at 37°C. Cultures were then incubated in blocking buffer (BB) (3% BSA, 22% polyvinyl pyrrolidone, 0.2% Triton X-100 in PBS) for 2 h, washed with PBS, and incubated with the YL 1/2 mAb that recognizes tyrosinated α-tubulin (1:200 in BB Serotec Ltd., Oxford, England), and/or the rabbit polyclonal Sup Glu antibody that recognizes detyrosinated α-tubulin (a kind gift from Dr. J. C. Bulinski; 1:200 in BB) for 2 h. Cultures were then washed in PBS and incubated with fluorescein or rhodamine conjugated secondary antibody (multiple labeling grade; Jackson ImmunoResearch Labs., Inc., West Grove, PA 1:30 in BB), and/or rhodamine-phalloidin (Molecular Probes, Eugene, OR; 3.3 μM in PBS containing 1% Tween 20) for 1 h. All preparations were washed in PBS and mounted on slides in citifluor (Citifluor Ltd., City University, London). Matched YL 1/2 and Sup glu images were collected as described below in "F-actin quantification." The distance between the most distally detected Sup glu staining and the most distally detected YL 1/2 staining was measured directly off the video screen by comparing the matched images.

Published May 15, 1993

Double Labeling with Rhodamine-Phalloidin and FITC or DTAF

Cultures treated with collapsing factor for varying lengths of time were fixed in PBS containing 4% paraformaldehyde and 10% sucrose for one hour or more, rinsed in PBS containing 100 mM glycine, and incubated for 1 h with rhodamine-phalloidin (3.3 μM in PBS containing 1% Tween 20). A fresh 1% solution of FITC (Sigma) or DTAF (5-[4,6-Dichlorotriazin-2-yl]aminofluorescein from Sigma) in DMSO was diluted 1,000-fold with vigorous vortexing into PBS immediately before use. Preparations were stained for 15 min, rinsed in PBS, and then mounted in gelvatol on slide glass.

F-actin Quantification

Images were acquired according to the methods of Redmond and Zigmond (1993). Growth cones were viewed on a standard epifluorescent microscope (Carl Zeiss) with a Zeiss 100× objective (1.25 ND), and a Quantex QC-100 camera (Quantex Corp., Sunnyvale, CA). Illumination was provided by a 100 W mercury arc lamp. Matched rhodamine-phalloidin and fluorescein images of each growth cone were digitized and corrected for both background and shading using an Image-1 processing system (Universal Image Corp., Media, PA). The light source intensity, gain, and black level setting on the Image-1 system and the intensifier settings on the Quantex camera were adjusted for each channel at the beginning of each experiment so that the maximal pixel intensities in all regions of the growth cone were within the dynamic range of the system. The range of absolute pixel intensities of both fluorophores in the cells was within the linear range of their respective quantum yield curves (based on plots of concentration of FITC, DTAF, and rhodamine-phalloidin blotted onto nitrocellulose versus absolute pixel intensity). The pixel intensities in the digitized images from the rhodamine channel are therefore proportional to the amounts of F-actin in those locations (Howard and Oresajo, 1985; Symons and Mitchison, 1991). The matching intensities of DTAF or FITC in the fluorescein channel were assumed to be proportional to the total amount of protein in the same locations.

The following procedure was used to obtain the average rhodamine-phalloidin signal, DTAF signal, and their ratio within a growth cone. A digital mask corresponding to the growth cone outline was generated from the rhodamine image. The sum of all background corrected rhodamine intensities within the masked area was then determined. The sum of all background corrected DTAF intensities was then determined within the same masked area. The summed rhodamine and fluorescein intensities were then divided by the area of the mask to generate separate average intensity values. The rhodamine-phalloidin to DTAF ratio was calculated using the same summed intensities.

Ratio images of the phalloidin to fluorescein signals were constructed from matched background subtracted rhodamine-phalloidin and DTAF images. Ratio images and pixel histograms of the digitized images were generated using Image-1 resident functions.

Statistical Methods

All statistical discriminations were made by the Wilcoxon rank test. This non-parametric test makes no assumptions about the statistical properties of the data sets. Its result is the probability that two sets of data could be drawn from the same population of values. Probabilities expressed in the Tables are for two-tailed determinations.

Preparation of Collapsing Factor

Collapsing factor was prepared as described previously (Raper and Kapfhammer, 1990) with significant modifications. Briefly, adult chicken brain membranes were solubilized in PBS containing 2% CHAPS buffered to pH 7.4 with 10 mM Tris. The extract was cleared by centrifugation for 1 h at 100,000 *g* and then passed through a Q-Sepharose (Pharmacia Fine Chemicals, Piscataway, NJ) anion exchange column. The flow-through was then loaded onto a S-Sepharose cation exchange column and eluted with PBS containing 0.9 M NaCl, 0.2% CHAPS, and 10 mM Tris, pH 7.4. This gives an eluate 10-fold enriched for collapsing activity. This material was then bound to WGA and eluted with 100 mM NaCl, 20 mM Na_2HPO_4, pH 7.2, 1 mM EDTA, 5% glycerol, and 0.5 M *N*-acetyl-d-glucosamine. This gives an eluate 500-fold enriched for collapsing activity. The eluate was stored at −70°C before use. The concentration of collapsing factor at which 90% of DRG growth cones collapsed was determined for each batch of enriched factor, and it was this concentration that was used throughout this study.

Results

Growth Cone Behavior during Collapse

Growth cones from DRG explants were examined using time-lapse video microscopy before and during treatment with the brain-derived collapsing factor. Care was taken to select only those growth cones that were not in contact with other axons or growth cones. Individual growth cones were observed by video microscopy for up to 30 min before the addition of collapsing factor. This ensured that they were growing in a consistent manner without spontaneous retractions. Before addition of the factor, growth cones generally have wide-spread lamellipodia and ten or more filopodia. Over a period of 7 min, filopodia are observed to extend, retract, bend along their length, and swing freely in the medium (Fig. 1, *A–C*). The shapes of the lamellipodia change over time. Some lamellipodia extend and a few lamellipodia retract while the body of the growth cone advances at 50–70 μm/h. Within a minute after adding the collapsing factor to the medium, lamellar protrusion ceases (13/15 growth cones), and as a consequence the body of the growth cone ceases to advance. Filopodia stop swinging and appear to be immobilized on the substrate. At the same time, both lamellipodia and filopodia start to retract (Fig. 1, *D* and *E*). In the next 10–70 min, the filopodia become shorter and fewer; the lamellipodia shrink back from the sides of the growth cone and form a phase dense stump (Fig. 1, *F–H*). In 8 of 15 growth cones filmed, varicosities in filopodia were seen to stream back towards the center of the collapsing growth cone at a rate on the order of 10 μm/min (Fig. 2, *arrowhead*). Our impression is that varicosities are most evident when the filopodia are very well attached to the substratum. Sometimes similar varicosities can be seen to move in a retrograde direction in the filopodia of untreated growth cones, but we do not know if they are related to those we see in collapsing growth cones.

A small number of filopodia are sometimes seen to extend during collapse at the same time as a majority of filopodia are immobilized or retracting (Fig. 3). In 5 of 15 cases filmed, during the initial 7 min of collapse, a small number (one to three) of filopodia extended forward rapidly at 10–18 μm/min. This rate is comparable to the most rapidly extending filopodia found in control growth cones. These unusual, rapidly extending filopodia (Fig. 3, *arrowhead*) are dramatically distinctive from their nearly immobile neighbors. The advancing filopodia stain with rhodamine-phalloidin and therefore contain F-actin (not shown). We have not observed them to stain with YL 1/2, and it therefore appears that they do not contain microtubules.

Growth Cone Behavior during Cytochalasin Treatment

The initial response of growth cones to cytochalasin B (2 μM) is similar to their response to the collapsing factor. Within 1 min after the addition of cytochalasin, lamellipodia stop protruding, and filopodia are immobilized. Both filopodia and lamellipodia retract (Fig. 4). As a result, lamellipodia become smaller, and filopodia become shorter and fewer (compare Fig. 4, *E* and *G*). Filopodial varicosities can be seen to be transported centripetally. Although collapse induced by cytochalasin is nearly indistinguishable from that induced by the collapsing factor, we noticed one difference.

Published May 15, 1993

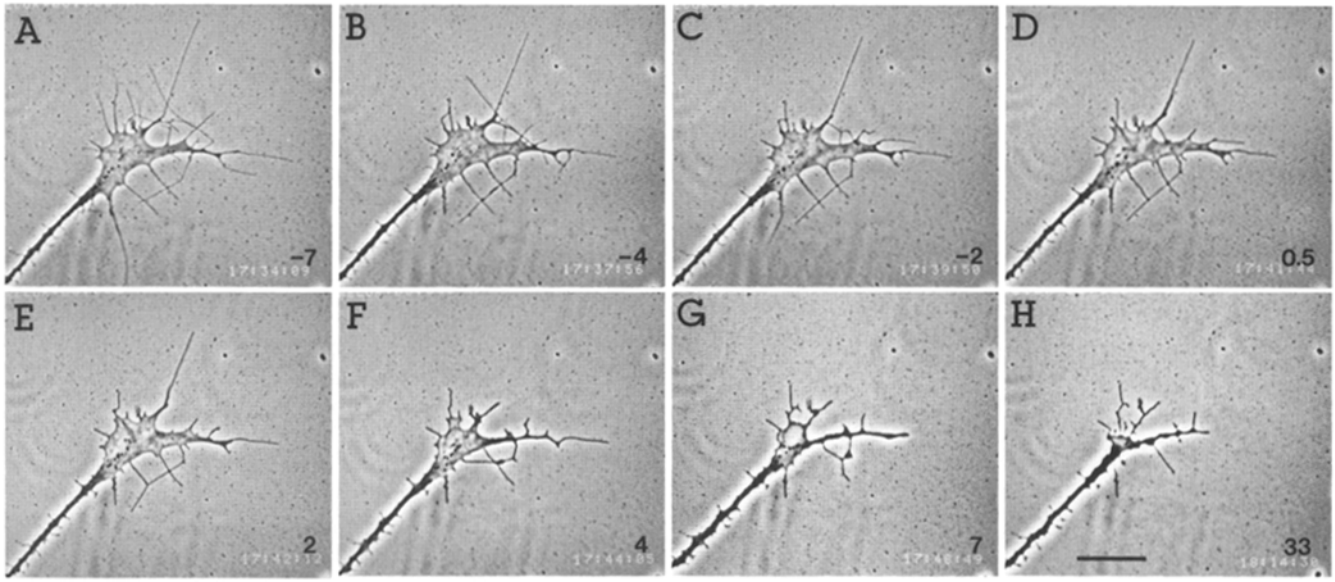

Figure 1. Time-lapse video images of a DRG growth cone before and after the addition of 500-fold–enriched collapsing factor. The time each frame was taken is indicated in the lower right hand corner of each panel. Negative numbers are minutes before the addition of collapsing factor (*A–C*) and positive numbers are minutes after addition (*D–H*). Bar, 20 μm.

There is a slow (8–12 μm/h) advancement of the growth cone tip during prolonged exposure to cytochalasin B (Marsh and Letourneau, 1984; Bentley and Toroian-Raymond, 1986) that is never seen with collapsing factor.

Distribution of F-actin and Microtubules during Collapse

The distributions of F-actin and microtubules were examined before and after treatment with collapsing factor. Growth cones were treated with collapsing factor for 0, 5, and 10 min and then fixed and stained with rhodamine-phalloidin to visualize F-actin, and YL 1/2 antibody to visualize tyrosinated α-tubulin. Fig. 5 shows a representative growth cone stained with phalloidin (column A) and YL 1/2 (column B) for each time point.

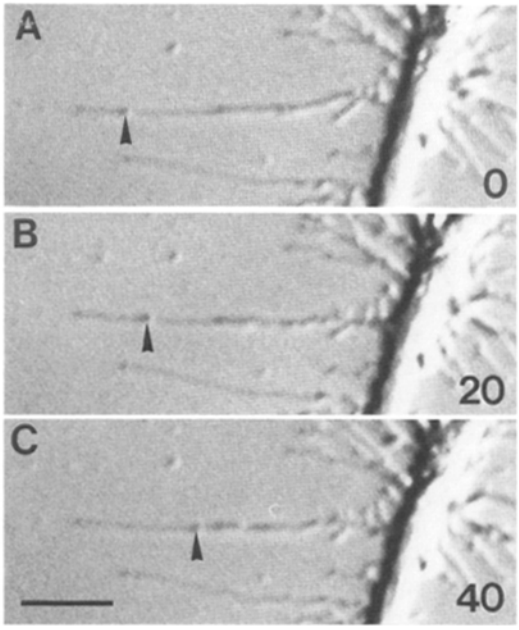

Figure 2. Retrograde translocation of a filopodial varicosity after a 5-min exposure to 10-fold–enriched collapsing factor. The arrow indicates the moving varicosity in each frame. Time in seconds relative to the first frame is indicated in the lower right hand corner of each panel. Bar, 8 μm.

F-actin extends throughout the lamellipodia and the filopodia of control growth cones (A0). In most cases, F-actin appears most dense near the leading edges and less dense in the growth cone center. Microtubules (B0) are tightly bundled within the axon and then splay out within the lamellipodia. The distal-most tips of the microtubules are found near the leading edges of the lamellipodia, and only occasionally enter the proximal portions of filopodia. Since most of the distal tips of microtubules are near the leading edges of lamellipodia, it is possible to predict their approximate distal-most extent from phase images of normal growth cones. Lamellipodia shrink in size after increasingly longer exposures to collapsing factor. F-actin is still present throughout the remaining lamellipodia and the filopodia (A5, A10). Microtubules are found to be increasingly bundled together in appearance in distal regions of growth cones (B10), particularly after 20 min or more exposure to collapsing factor (not shown). The tips of microtubules then tend to end close to the distal most extent of the neurite.

These time series experiments show that microtubules extend to the leading edges and F-actin fills the outer rims of both control and collapsing growth cones. Unfortunately, a population study of growth cones exposed to collapsing factor leaves many questions unanswered. With respect to the microtubules, for example, might the growth cone have collapsed as microtubules retreated, or might the collapsed morphology develop as a bundle of promiscuously polymerizing microtubules pushes out from the front of the growth cone?

To examine whether microtubules retract or advance during collapse, we followed the behavior of individual growth

Published May 15, 1993

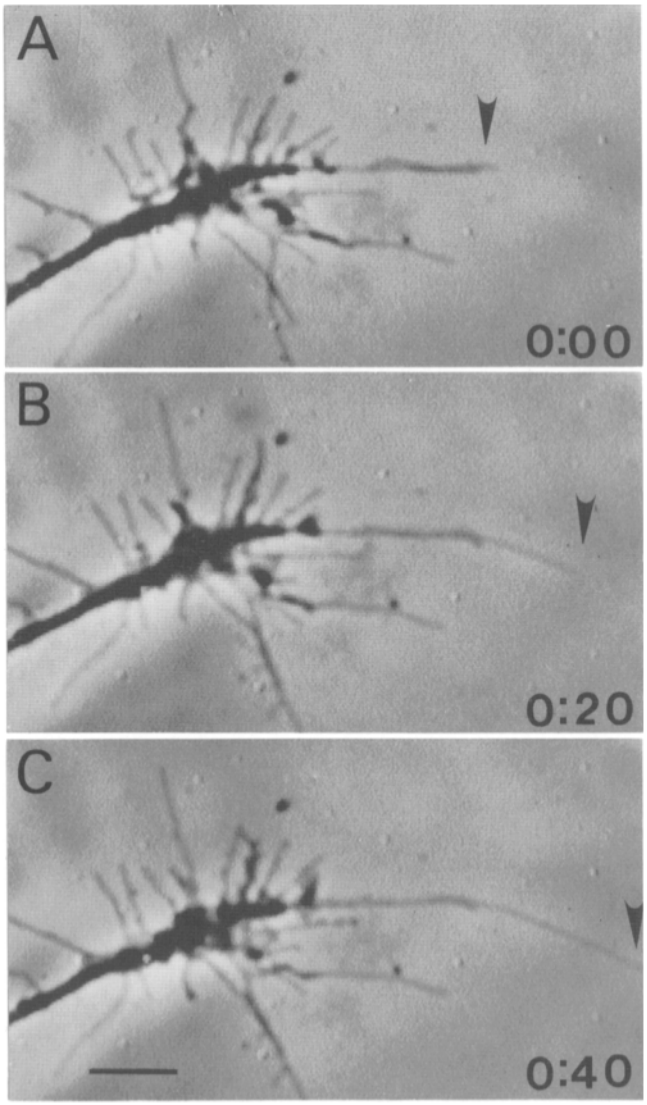

Figure 3. Rapidly extending filopodium from a growth cone exposed to a 10-fold enriched collapsing factor for 2.5 min. The arrow indicates the distal-most tip of the filopodium. Note that the other filopodia do not extend appreciably during this time period. The average measured rate of extension between *A* and *C* is 30 μm/min. Time in seconds relative to the first frame is indicated in the lower right hand corner of each panel. Bar, 10 μm.

cones before and during the initial stages of collapse using time-lapse videomicroscopy. We then fixed each growth cone and double-stained it for F-actin and microtubules. The approximate distal-most extent of the microtubules in the growth cones before collapse was predicted from the phase images (as described above). We could then compare the absolute positions of the microtubules in the same growth cone before and during partial collapse.

The results from one growth cone are shown in Fig. 6. The phase image of a growth cone was outlined just before the addition of collapsing factor (Fig. 6 *A*, *shaded*) and 7 min after the addition of collapsing factor (Fig. 6 *A*, *solid*). The growth cone was then fixed and double stained for F-actin (Fig. 6 *B*, *solid*) and microtubules (Fig. 6 *C*, *solid*). We would predict that the distal-most tips of microtubules are near the leading edges of the lamellipodia in the uncollapsed growth cone. This is within 3 μm of their actual distal-most position after partial collapse. The average distance between the estimated positions of the distal-most microtubules before collapse and their position during partial collapse in six growth cones ranged from an apparent withdrawal of −6 μm to an apparent advance of +3 μm. The average difference was −2.4 μm. These results suggest to us that microtubules neither polymerize nor depolymerize to any great extent during the early stages of collapse.

Distribution of Microtubule Isoforms during Collapse

To assay for the effect of collapsing factor on the dynamics of microtubule assembly, the distributions of tyrosinated and detyrosinated forms of microtubules in control and treated growth cones were examined. The α-tubulin in recently polymerized microtubules is tyrosinated (Kumar and Flavin, 1981; Thompson, 1982; Gordon-Weeks and Lang, 1988). As the growth cone moves on, the tyrosinated α-tubulin in newly polymerized microtubules is gradually converted to the detyrosinated form (Lim et al., 1989; Robson and Burgoyne, 1989; Arregui et al., 1991; Mansfield and Gordon-Weeks, 1991). It is therefore possible to determine where the most recently polymerized microtubules are by comparing the distributions of the tyrosinated and detyrosinated forms. If the collapsing factor stimulates the polymerization of microtubules, the proportion of tyrosinated as compared to detyrosinated microtubules should increase in affected growth cones. The distance between the distal tips of microtubules containing only tyrosinated α-tubulin and those containing tyrosinated α-tubulin and detyrosinated α-tubulin should increase. Similarly, if the collapsing factor inhibits the polymerization of microtubules, the proportion of tyrosinated microtubules in affected growth cones should decrease. Then the distance between the distal tips of microtubules containing only tyrosinated α-tubulin and those containing detyrosinated α-tubulin should decrease.

Growth cones were double labeled with YL 1/2 antibody to visualize tyrosinated α-tubulin and the Sup glu antibody to visualize detyrosinated α-tubulin. Fig. 7 shows the staining patterns for YL 1/2 (Fig. 7 *A*) and Sup glu (Fig. 7 *B*) in a control growth cone, and YL 1/2 (Fig. 7 *C*) and Sup glu (Fig. 7 *D*) in a growth cone exposed to collapsing factor for 5 min. As expected, in control growth cones, the microtubules in lamellipodia contain tyrosinated α-tubulin, while the bundled microtubules in the axon shaft contain both tyrosinated and detyrosinated α-tubulin (Fig. 7, *A* and *B*). The same pattern is evident in growth cones treated with collapsing factor for 5 min (Fig. 7, *C* and *D*). Similar staining patterns have been observed in growth cones treated with collapsing factor for even longer periods of time (10 and 30 min, not shown). In one experiment we measured the distance between the distal most tips of tyrosinated microtubules as visualized with the YL 1/2 antibody, and the distal-most tips of detyrosinated microtubules as visualized with Sup glu antibody (Table I). The average distances between the two isoform distributions were not significantly affected by treatment with collapsing factor for either 5 or 30 min. These results suggest that the rates of net tubulin polymerization are not significantly affected by the collapsing factor.

Changes in Relative F-actin Concentration during Collapse

We then examined the distribution of F-actin in growth cones

Published May 15, 1993

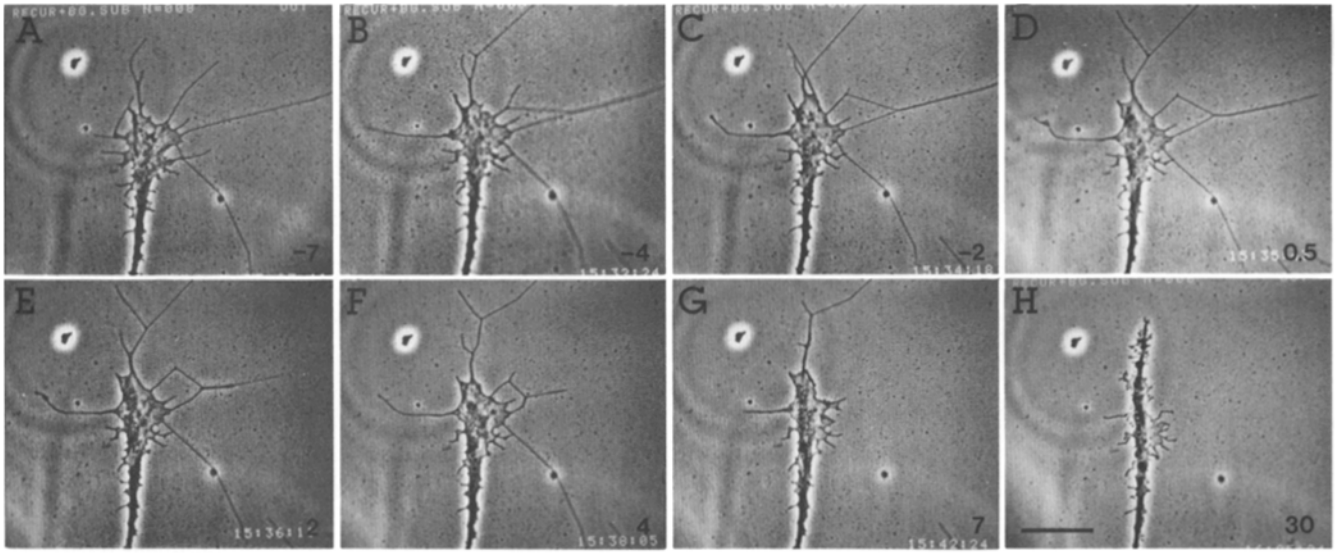

Figure 4. Time-lapse video images of a growth cone before and after addition of 2 μM cytochalasin B. Although the growth cone collapses in the presence of cytochalasin B, it continues to advance very slowly. The time each frame was taken is indicated in the lower right hand corner of each panel. Negative numbers are minutes before the addition of cytochalasin (*A–C*) and positive numbers are minutes after addition (*D–H*). Bar, 20 μm.

before and during collapse. We measured the proportion of total protein comprised by F-actin in control as compared to partially collapsed growth cones. This was accomplished by ratioing the fluorescence intensity of rhodamine–phalloidin to the fluorescence intensity of a general protein marker (either DTAF or FITC). Higher ratios of phalloidin to DTAF indicate higher proportions of F-actin to all proteins. We have therefore called this proportion the "relative concentration" of F-actin.

We examined the average relative concentrations of F-actin in control growth cones and growth cones treated with collapsing factor for 5 min. The average rhodamine–phalloidin intensities corresponding to F-actin increased only slightly in collapsing growth cones, while the average DTAF intensities corresponding to general protein increased by a factor of more than twofold (Table II). This implies that as growth cones collapse: their spread area decreases, the thickness of the remaining portion therefore increases, and the F-actin content in the remaining portion is nearly unchanged. The result is a decrease in the proportion of F-actin as compared to all proteins in collapsing growth cones. This result is consistent with a loss of F-actin in the growth cone as a whole during the early stages of collapse.

We next examined the spatial distributions of F-actin concentrations in control and collapsing growth cones. The staining patterns of rhodamine–phalloidin, DTAF, and the ratio images of rhodamine to DTAF are shown in Fig. 8 for both a control growth cone and a growth cone treated with collapsing factor for 5 min. The bar on the bottom gives a calibration for the pseudocolor representation. Warm colors represent higher relative concentrations of F-actin. The control growth cone has relatively higher rhodamine intensities in filopodia and near the leading edges of lamellipodia as compared to the growth cone center. DTAF intensities are relatively low in filopodia and the leading edges of lamellipodia, and higher in the center of the growth cone. The ratio image therefore shows a high relative concentration of F-actin in filopodia and the leading edges of lamellipodia, and low concentrations in the center of the growth cone. In contrast, the growth cone treated with collapsing factor for 5 min has significantly lower relative concentrations of F-actin at the growth cone's periphery compared to controls, while the center is less affected.

Fig. 9 shows the intensity profiles for each image in Fig. 8. The profiles correspond to lines that run from the center to the leading edges between the indicated crosses. In the control growth cone, the rhodamine fluorescence intensity in the leading edge is about three times as high as in the center of the growth cone. The FITC fluorescence intensity in the leading edge is half that in the center of the growth cone. The ratio shows the F-actin concentration in the leading edge is about six times that in the center. In the growth cone treated with collapsing factor, the difference between relative F-actin concentrations at the edge and the center is significantly reduced.

In each of four independent experiments, matched rhodamine–phalloidin and DTAF (or FITC) images were collected for 15–20 control growth cones and the same number of growth cones exposed to collapsing factor for 5 min (see Table III). Ratio images were computed for each growth cone and then analyzed. In one analysis, the apparent relative concentration of F-actin at each pixel value was tabulated and used to generate a curve for each growth cone. Each curve in Fig. 10 (*A* and *B*) represents the proportion of a growth cone's area indicated on the y-axis that has F-actin concentrations lower than the indicated amount on the x-axis. Curves shifted to the right contain higher actin concentrations and curves shifted to the left have lower concentrations. Although there is considerable variability from growth cone to growth cone, the curves for the collapsing factor treated growth cones are clearly shifted towards lower relative F-actin concentrations (Fig. 10 *B*) as compared to the control curves (Fig. 10 *A*). Fig. 10 *C* shows the proportion of growth cone areas that have the indicated F-actin concentrations for all the

Published May 15, 1993

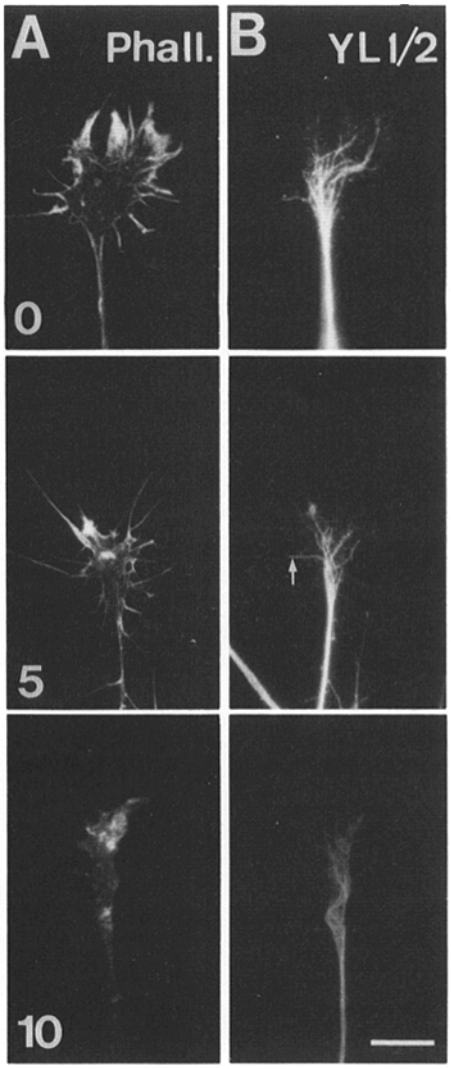

Figure 5. Distribution of F-actin and microtubules in control and collapsing factor–treated growth cones. Growth cones were treated with 500-fold–enriched collapsing factor. Growth cones representative of those found at 0, 5, and 10 min after the addition of collapsing factor are shown. Cultures were double labeled with rhodamine–phalloidin to visualize F-actin (*A0, 5,* and *10*) and YL 1/2 antibody to visualize microtubules (*B0, 5,* and *10*). An arrow in A5 indicates a microtubule entering a filopodium. Bar, 10 μm.

growth cones in the control and treated conditions for the same experiment. The control values range from low to high relative F-actin concentrations, while the values for the treated growth cones range from low to moderate concentrations.

Table III summarizes the changes in relative F-actin concentrations observed in collapsing as compared to control growth cones in four experiments. For each experiment the average reduction in F-actin concentration is indicated for those regions of the growth cone that contain the lowest (10th percentile), the median (50th percentile), and highest (90th percentile) concentrations of F-actin. The 10th percentile values correspond to low F-actin concentrations that are representative of the center of the growth cones, while the 90th percentile values correspond to high F-actin concentrations that are representative of the peripheral regions of the

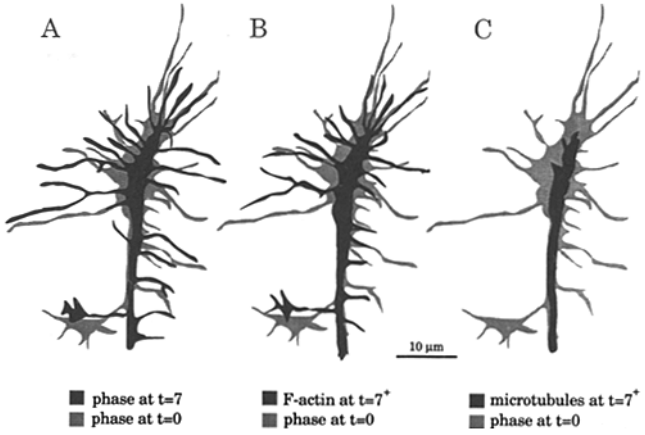

Figure 6. Tracings of time-lapse video images of a single growth cone before the addition of collapsing factor (*A, grey*) and 7 min after the addition of 10-fold enriched collapsing factor (*A, solid*). The growth cone was fixed just after the last image in A and double labeled with rhodamine-phalloidin to visualize F-actin (*B, solid*) and YL 1/2 antibody to visualize microtubules (*C, solid*). The fluorescent images are superimposed on the untreated phase image for reference.

growth cones. The 90th percentile values are consistently reduced to 60–70% of their control values by treatment with collapsing factor, a very significant decrease. A significant decrease is also observed in the median F-actin concentrations of treated growth cones. The 10th percentile values are reduced by collapse factor treatment by a small or possibly insignificant degree. These results indicate that the relative F-actin concentrations are greatly reduced in the growth cone periphery during collapse without there being a compensatory rise in F-actin concentrations in the growth cone center.

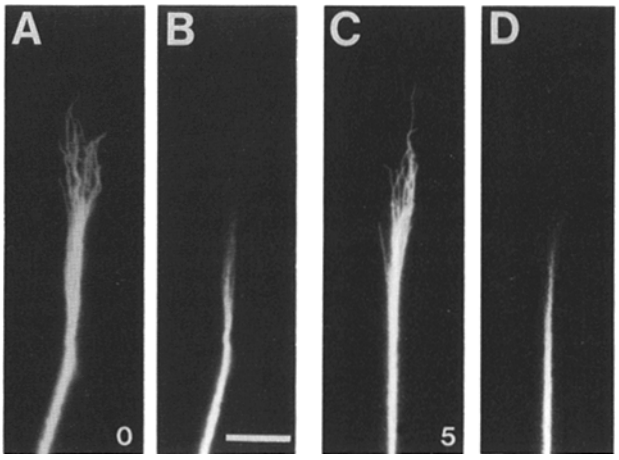

Figure 7. Distributions of microtubule isoforms in growth cones before and after treatment with collapsing factor. Growth cones were double labeled with YL 1/2 to visualize tyrosinated microtubules, and Sup Glu to visualize detyrosinated microtubules. (*A*) Tyrosinated microtubules and (*B*) detyrosinated microtubules in an untreated growth cone. (*C*) Tyrosinated microtubules and (*D*) detyrosinated microtubules in a growth cone treated with 10-fold–enriched factor for 5 min. Bar, 10 μm.

Published May 15, 1993

Table I. Distance between Tips of Tyrosinated and Detyrosinated Microtubules in Control and Collapsing Factor-treated Growth Cones

Treatment time		Distance ± SEM
(*min*)	(*n*)	(*μm*)
0	115	5.4 ± 0.2
	79	4.4 ± 0.2
5	116	4.5 ± 0.2
	21	5.1 ± 0.4
30	124	5.9 ± 0.3
	44	4.1 ± 0.5

The distance between the distal tips of microtubules containing only tyrosinated α-tubulin and those containing tyrosinated α-tubulin and detyrosinated α-tubulin in collapsing factor treated growth cones. Growth cones treated for 0, 5, and 30 min with collapsing factor were double labeled with the YL 1/2 antibody to visualize tyrosinated microtubules and the Sup glu antibody to visualize detyrosinated microtubules. The distances between the distal-most extents of the two isoforms were measured as described in Materials and Methods. Each line repesents the data from a separate culture. If the two values for each time point are consolidated together, there is no statistically significant difference between untreated and treated growth cones according to the nonparametric Wilcoxon rank test.

Discussion

Normal growth cone motility requires that there be a balance between the polymerization and depolymerization of both F-actin and microtubules. If this balance is disturbed then normal growth cone structure is altered and extension can fail. Previous studies have shown that the inhibition of actin polymerization, excessive microtubule polymerization, or microtubule depolymerization can all inhibit growth cone extension (Yamada et al., 1970; Letourneau and Ressler, 1984; Letourneau et al., 1987; Gordon-Weeks et al., 1989; Keith, 1990). Growth cone collapse that is induced by our brain derived collapsing factor could theoretically work through any one of these mechanisms. Alternatively, it could be caused by the translocation of F-actin or microtubules towards the growth cone center. Our results indicate that the presence of collapsing factor is associated with a net loss of F-actin. We hypothesize that the collapse of growth cone structure is caused by this loss of F-actin.

Table II. Comparison of F-actin Content in Control and Collapsing Growth Cones

		Rho-Phalloidin	DTAF	Ratio
	(*n*)			
Exposure 3				
Control	21	14.0 ± 1.2	13.7 ± 1.6	1.11 ± 0.09
Treated	17	19.1 ± 3.3	39.8 ± 4.4	0.49 ± 0.05
Change		36%	191%**	−56%**
Exposure 4				
Control	25	14.8 ± 0.8	5.7 ± 0.4	2.79 ± 0.18
Treated	23	16.9 ± 0.8	12.7 ± 0.9	1.42 ± 0.08
Change		14%	123%**	−49%**

F-actin and general protein content in normal and collapsing growth cones. Shown are the average intensities of the rhodamine-phalloidin signals, the DTAF signals, and the ratios of the phalloidin to DTAF signals for groups of control growth cones and growth cones treated for 5 min with collapsing factor. As described in the text, the ratio of phalloidin to DTAF is interpreted as a measurement of the relative F-actin concentration. The concentration of F-actin is seen to decrease during collapse. All units are arbitrary but are consistent within each experiment. Changes marked ** are statistically significant to the $P < 0.01$ level as determined by the nonparametric Wilcoxon rank test.

Our results are not consistent with a model that depends on changes in microtubule polymerization or depolymerization as a basis for factor induced growth cone collapse. If the collapsing factor causes microtubules to polymerize promiscuously, then we would expect to find looped microtubules in collapsing growth cones analogous to those seen after micromolar taxol treatment, or an unusually large accumulation of tyrosinated microtubules in collapsing growth cones as the α-tubulin pool is polymerized (Letourneau and Ressler, 1984; Gordon-Weeks et al., 1989; Mansfield and Gordon-Weeks, 1991). We might also have expected the leading edge of the growth cone to lunge forward as excess microtubules are generated. We did not observe any disorganization of microtubule structure during the early stages of collapse when individual microtubules can be visualized at the light level. Microtubules were straight and their tips were clearly visible, in contrast to the densely packed, long, tangled, and looped appearance of microtubules in taxol treated growth cones (Letourneau and Ressler, 1984; Mansfield and Gordon-Weeks, 1991). The relative distributions of newly polymerized tyrosinated α-tubulin and the less recently polymerized detyrosinated isoform resembled control distributions even in fully collapsed growth cones. We observed no lunge forward of microtubules in collapsing growth cones or of the collapsing growth cones themselves. It is therefore unlikely that overpolymerization of microtubules is the cause of factor induced collapse.

Similarly, it is unlikely that abnormal depolymerization of microtubules is the cause of factor induced growth cone collapse. If the collapsing factor causes microtubules to depolymerize, then we would have expected the distal-most tips of microtubules to retreat backwards during collapse. We might also have expected a comparative decrease in the amount of tyrosinated microtubules as polymerization was inhibited. We did not detect a reproducible retreat of microtubules during collapse. The distal-most tips of microtubules in collapsing growth cones are very near their predicted positions before collapse. The relative distributions of newly polymerized tyrosinated tubulin and the detyrosinated isoform associated with older microtubules resembled control distributions. These results argue against a factor induced depolymerization of microtubules.

These results suggest to us that the rearrangement of microtubules in collapsing growth cones may be passive in nature. We speculate that microtubules are squeezed into the midline of the growth cone as it shrinks during collapse. However, we can not rule out the possibility that an active process, perhaps the cross-linking of microtubules, may cause their apparent bundling. Our failure to detect any advancement of growth cones treated with collapsing factor, in contrast to their very slow advancement in the presence of cytochalasin B, suggests that the loss of F-actin alone can not explain all of the effects of the collapsing factor. Exposure to collapsing factor may have additional effects on growth cones that explain their failure to advance, for example, axonal transport may be inhibited or microtubules may be cross linked or capped.

There are at least two different ways in which actin reorganization might drive growth cone collapse. Actin might simply depolymerize, leaving the cell membrane unsupported and unable to hold its normal shape. Alternatively, the same shape change might occur if actin remains polymerized but

Published May 15, 1993

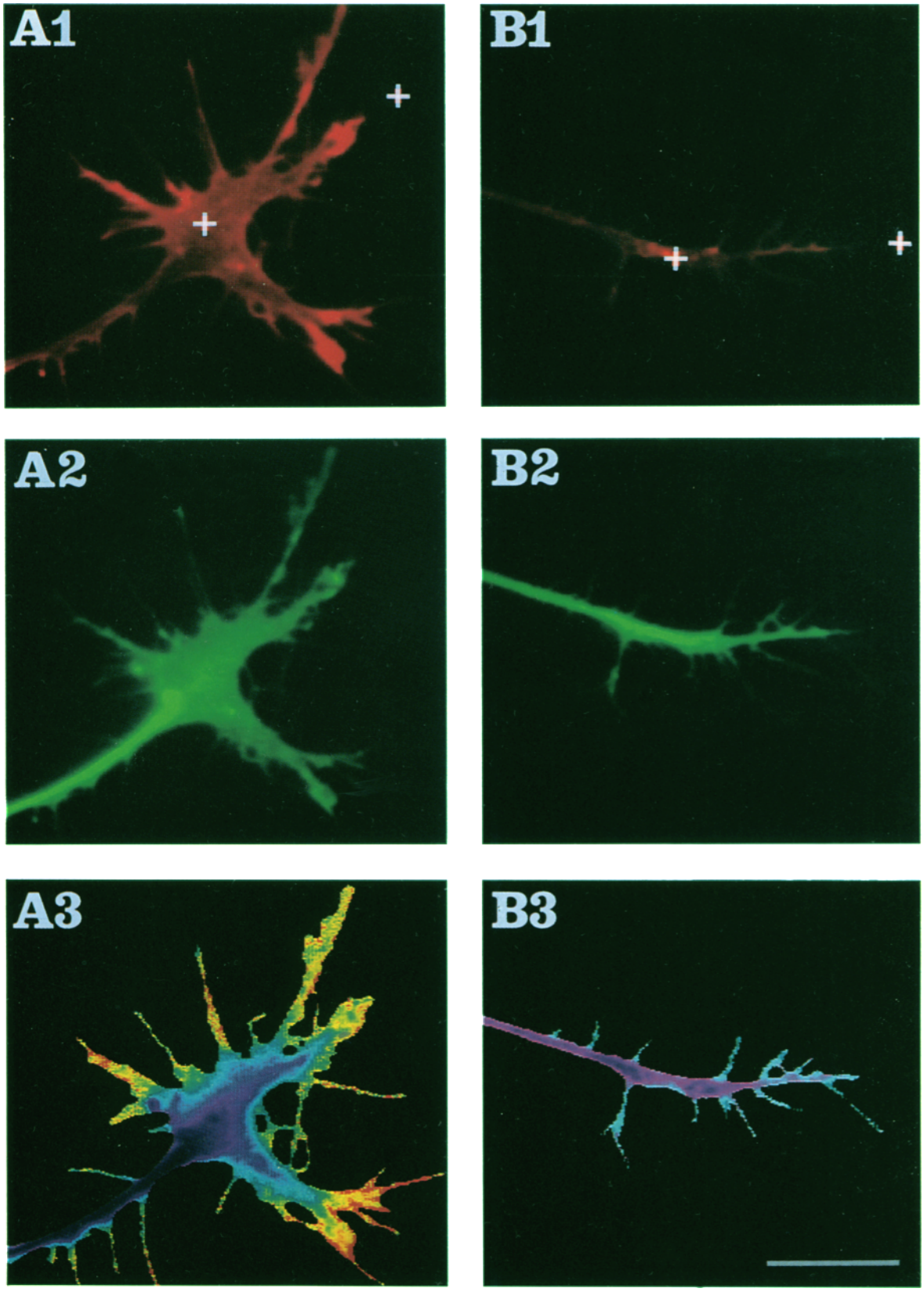

Figure 8. The spatial distributions of F-actin in normal and 500-fold-enriched collapsing factor treated growth cones. Growth cones were fixed and double labeled with rhodamine-phalloidin and DTAF. The ratios of the rhodamine and DTAF images were then constructed to visualize the spatial distributions of high and low F-actin concentrations in a control growth cone (*A*) and a growth cone treated for 5 min with 500-fold-enriched collapsing factor (*B*). (*A1* and *B1*) Rhodamine-phalloidin staining; (*A2* and *B2*) DTAF staining; (*A3* and *B3*) ratio image of rhodamine-phalloidin to DTAF. A color key for the ratios of rhodamine to DTAF is shown below. Bar, 20 μm.

Published May 15, 1993

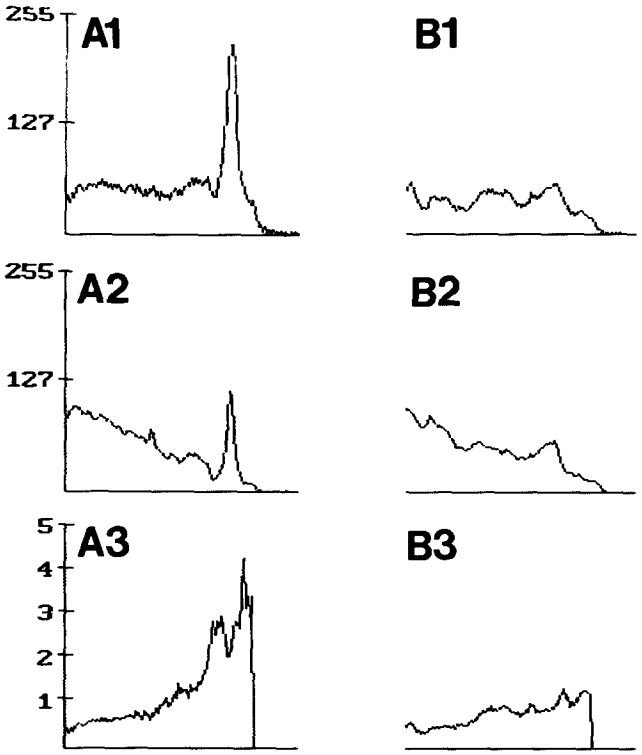

Figure 9. F-actin concentrations in the leading edges and centers of control growth cones (*A1–3*) and growth cones treated with collapsing factor for 5 min (*B1–3*). Intensity profiles were generated for each image in Fig. 8 from the crosses in the center of each growth cone to the crosses at the distal edges indicated in A1 and B1. (*A1* and *B1*) Rhodamine-phalloidin; (*A2* and *B2*) DTAF; (*A3* and *B3*) Ratio of rhodamine-phalloidin to DTAF. The scales in A1 and A2 represent the relative pixel intensities, and in A3 the ratio values.

is translocated into a condensed ball in the center of the growth cone. Translocation might be the result of cortical contraction of actin fibrils or the overstimulation of the normal process that causes F-actin to translocate towards the center of the growth cone. If the collapsing factor causes a net loss of F-actin, then the concentration of F-actin inside a collapsing growth cone should be lower than normal. If the factor induces F-actin translocation, then F-actin will be redistributed but its overall concentration within the growth cone should remain unchanged.

Table III. Summary of Changes in F-actin Concentration after a 5-min Exposure to Collapsing Factor

	N_{con}/N_{exp}	10th percentile	50th percentile	90th percentile
Exposure				
1	15/21	−23%*	−36%**	−40%**
2	20/13	−20%	−28%**	−31%**
3	19/18	−12%	−40%**	−45%**
4	24/20	−5%	−17%	−41%**

Summary of F-actin concentration changes after a 5-min exposure to collapsing factor. The median concentrations of F-actin (50th percentile) for each growth cone were averaged within the control group and then compared to the average for the experimental group exposed to collapsing factor for 5 min. Similarly, the averages for the 10th and 90th percentiles were compared as well. The change in relative F-actin concentration is expressed as a percentage of the control value. Changes marked * and ** are statistically significant to the $P < .01$ and the $P < .001$ levels, respectively, as determined by the nonparametric Wilcoxon rank test.

An estimate of the amount of F-actin inside the growth cone as compared to all proteins was provided by comparing the fluorescent signal generated by rhodamine-phalloidin to that of DTAF or FITC. Rhodamine-phalloidin binds F-actin in a stoichiometric fashion and is commonly used to quantify F-actin (Howard and Oresajo, 1985; Cano et al., 1991; Symons and Mitchison, 1991). The non-specific protein stains DTAF or FITC served as standards (Crissman and Steinkamp, 1974; Crissman et al., 1985) to which the phalloidin signal could be compared. We presumed that their signals are proportional to all proteins in the growth cone. A high ratio of phalloidin as compared to a general protein stain would indicate a higher proportion, and therefore a higher relative concentration of F-actin present.

A normal, motile growth cone has a high relative concentration of F-actin within its lamellipodia and filopodia, and a lower relative concentration in its center. A growth cone treated with collapsing factor, even for a relatively short time, has a lower total concentration of F-actin. The apparent loss of F-actin is most dramatic in the periphery, and no region of the growth cone shows any compensating increase in F-actin. These results suggest there is a net loss of F-actin during collapse, rather than a rear-ward translocation into the growth cone center or global contraction of F-actin throughout the growth cone.

Does this net loss of F-actin cause growth cone collapse or is it merely associated with collapse? Supporting the hypothesis that it actually causes collapse is the observation that cytochalasin B, a drug known to block actin polymerization, also induces growth cone collapse. Cytochalasin is generally thought to cause net actin depolymerization by capping the ends of actin filaments (review by Cooper, 1987; but see Sampath and Pollard, 1991). Both collapsing factor and cytochalasin treatment immobilize filopodia and cause retraction of lamellipodia and filopodia. This similarity in growth cone response raises the possibility that factor induced collapse involves the net inhibition of actin polymerization, and loss of polymerized actin causes collapse.

The mechanism by which F-actin is lost during factor mediated collapse is unknown. Since the loss of F-actin is most dramatic in the lamellipodia and filopodia, and since the effects of collapsing factor are similar to that of cytochalasin, it is possible that this loss results from a failure to replace F-actin at the leading edge during normal actin recycling. This could occur if the collapsing activity induced the blockade of actin nucleation sites, the sequesterization of actin monomers, or a modification of actin that interferes with polymerization. However, we cannot rule out the possibility that actin polymerizes normally in collapsing growth cones but is depolymerized at an accelerated rate. This could occur if the collapsing activity induced a filament severing and capping activity or a modification of actin that facilitates depolymerization.

The treatment of growth cones with an ionophore that increases intracellular Ca^{2+} concentrations has been shown to cause growth cone collapse, perhaps by destabilizing the actin meshwork (Lankford and Letourneau, 1989). However, growth cone collapse induced by the brain derived collapsing factor is unlikely to be mediated by Ca^{2+} because there

Published May 15, 1993

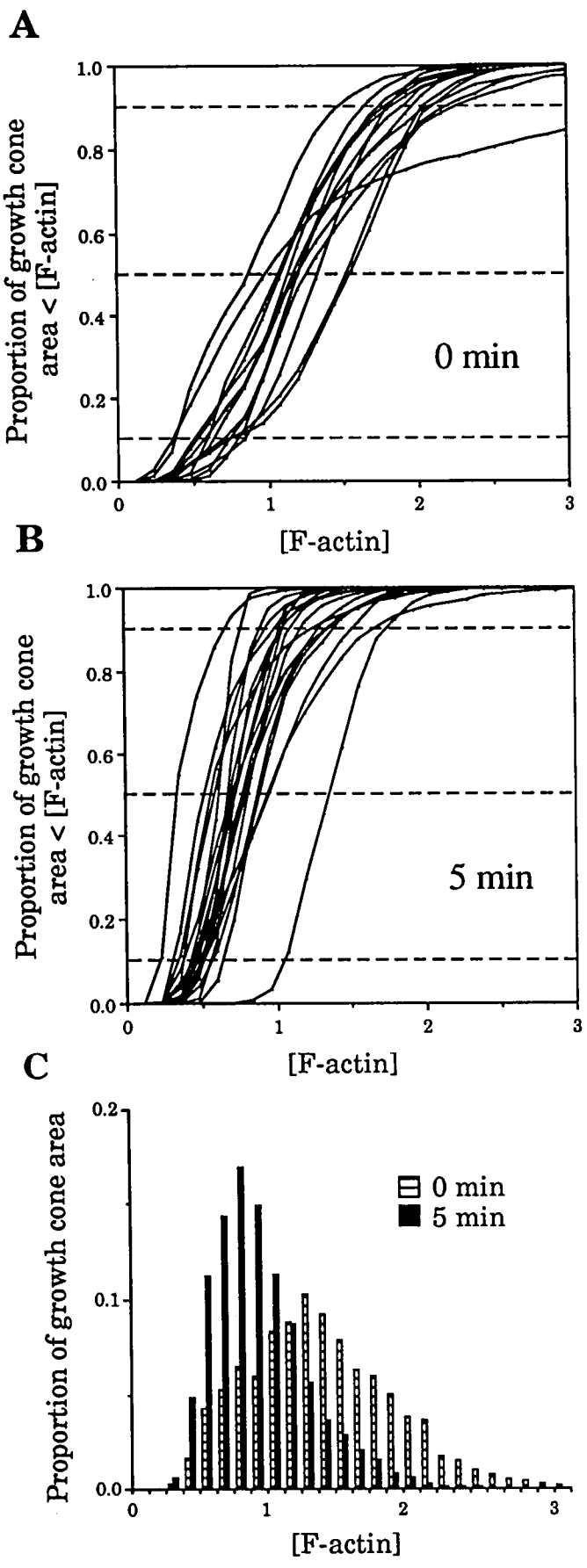

is no detectable change in internal-free calcium in growth cones during collapse (Ivins et al., 1991).

We were surprised to find a small number of filopodia in collapsing growth cones that advance at high rates while the lamellipodia and most other filopodia are slowly retracting. These rapidly extending filopodia contain F-actin as judged by rhodamine-phalloidin staining. They presumably represent discrete locations with active actin nucleation sites that have access to monomeric actin even during collapse. If one assumes that actin monomer is freely diffusible, then this would tend to argue against the sequesterization or modification of actin as the mechanism responsible for the loss of F-actin during collapse.

Actin polymerization correlates temporally and spatially with lamellar protrusion in motile cells (Omann et al., 1987; Devreotes and Zigmond, 1988; Stossel, 1989; Cooper, 1991) and has been hypothesized to drive membrane advancement (Hill and Kirschner, 1982; Theriot et al., 1992). Our results suggest that a glycoprotein found in normal brains can induce a net depolymerization of actin in growth cones. In consequence, protrusion of the leading edge fails and the normal motile structure collapses. What is the normal function of the collapsing protein in the nervous system? We believe that it may act as a guidance cue that controls the direction of growth cone extension. In this light an important question is whether this depolymerization effect can be localized to a subregion of a growth cone when the collapsing signal is applied locally. If so, it would suggest an effective method of growth cone steering in which actin would depolymerize on one side of a growth cone while the opposite, unaffected side would continue advancing. Advance on the unaffected side might even accelerate if additional actin monomer were made available by depolymerization on the affected side. This kind of a push-pull mechanism has many attractive features for growth cone guidance.

We thank Sally Zigmond for many very helpful discussions, for use of her imaging equipment, and her helpful reading of the manuscript. We would also like to acknowledge Simon Goodman's help in some early pilot experiments for this project. Thanks also to Chlöe Bulinski for the Sup Glu antibody, Yuling Luo for the brain derived collapsing factor, and Janet Baird for the bovine pituitary extract.

Support for this work was provided by a grant from the National Science Foundation to J. A. Raper, the Medical Research Council to P. Gordon-Weeks, training grant T32-HD-07067 to J. Fan, and a travel grant from NATO.

Received for publication 20 October 1992 and in revised form 28 January 1993.

Figure 10. F-actin concentrations in control growth cones and growth cones exposed to 500-fold-enriched collapsing factor for 5 min. For the control group (n = 14), the percentage of each growth cone area that has an apparent F-actin concentration less than the indicated value is plotted (*A*). The same plot is shown for the experimental group (n = 19) in *B*. In these plots, curves shifted to the left represent lower overall F-actin concentrations, and curves shifted to the right represent higher overall F-actin concentrations. (*C*) The proportion of control growth cone areas at given F-actin concentrations (▤) and those of treated growth cones at given concentrations (■) for the same data set. Again, distributions shifted to the left indicate lower F-actin concentrations, curves shifted to the right represent higher F-actin concentrations. The apparent F-actin concentration is expressed in arbitrary linear units.

References

Arregui, C., J. Busciglio, A. Caceres, and H. S. Barra. 1991. Tyrosinated and detyrosinated microtubules in axonal processes of cerebellar macroneurons grown in culture. *J. Neurosci. Res.* 28:171–181.

Bamburg, J. R., D. Bray, and K. Chapman. 1986. Assembly of microtubules at the tip of growing axons. *Nature (Lond.).* 321:788–790.

Bentley, D., and A. Toroian-Raymond. 1986. Disoriented pathfinding by pioneer neurone growth cones deprived of filopodia by cytochalasin treatment. *Nature (Lond.).* 323:712–715.

Burmeister, D. Q., and D. J. Goldberg. 1988. Micropruning: the mechanism of turning of aplysia growth cones at substrate borders *in vitro*. *J. Neurosci.* 8(9):3151–3159.

Cano, M. L., D. A. Lauffenburger, and S. H. Zigmond. 1991. Kinetic analysis of F-actin depolymerization in polymorphonuclear leukocyte lysates indicates that chemoattractant stimulation increase actin filament number without altering the filament length distribution. *J. Cell Biol.* 115(3):677–687.

Chang, S., F. G. Rathjen, and J. A. Raper. 1987. Extension of neurites on axons is impaired by antibodies against specific neural cell surface glycoproteins. *J. Cell Biol.* 104:355–362.

Cooper, J. A. 1987. Effects of cytochalasin and phalloidin on actin. *J. Cell Biol.* 105:1473–1478.

Cooper, J. A. 1991. The role of actin polymerization in cell motility. *Ann. Rev. Physiol.* 53:585–605.

Crissman, H. A., Z. Darzynkiewicz, R. A. Tobey, and J. A. Steinkamp. 1985. Correlated measurements of DNA, RNA, and protein in individual cells by flow cytometry. *Science (Wash. DC).* 228:1321–1324.

Crissman, H. A., and J. S. Steinkamp. 1974. Rapid simultaneous measurement of DNA, protein, and cell volume in single cells from large mammalian cell populations. *J. Cell Biol.* 59:766–770.

Daniels, M. P. 1971. Colchicine inhibition of nerve fiber formation in vitro. *J. Cell Biol.* 53:164–176.

Devreotes, P. N., and S. H. Zigmond. 1988. Chemotaxis in eukaryotic cells: a focus on leukocytes and dictyostelium. *Ann. Rev. Cell Biol.* 4:649–686.

Egelhoff, T. T., and J. A. Spudich. 1991. Molecular genetics of cell migration: Dictyostelium as a model system. *Trends Genet.* 7:161–166.

Forscher, P., and S. J. Smith. 1988. Actions of cytochalasins on the organization of actin filaments and microtubules in a neuronal growth cone. *J. Cell Biol.* 107:1505–1516.

Gordon-Weeks, P. R. 1987. The cytoskeletons of isolated neuronal growth cones. *Neuroscience.* 21:977–987.

Gordon-Weeks, P. R. 1991. Evidence for microtubule capture by filopodial actin filaments in growth cones. *Neuro. Report.* 2:573–576.

Gordon-Weeks, P. R., and R. D. A. Lang. 1988. The α-tubulin of the growth cone is predominantly in the tyrosinated form. *Dev. Brain Res.* 42:156–160.

Gordon-Weeks, P. R., S. G. Mansfield, and I. Curran. 1989. Direct visualization of the soluble pool of tubulin in the neuronal growth cone: immunofluorescence studies following taxol polymerization. *Dev. Brain. Res.* 49:305–310.

Gundersen, R. W., and J. N. Barrett. 1980. Characterization of the turning response of dorsal root neurites toward nerve growth factor. *Dev. Biol.* 93:1–12.

Hamel, E. 1990. Interactions of tubulin with small ligands. *In* Microtubule Proteins. Avila, J., editor. CRC Press, Inc., Boca Raton, FL. 89–191.

Hammarback, J. A., J. B. McCarthy, S. L. Palm, L. T. Furcht, P. C. Letourneau. 1988. Growth cone guidance by substrate-bound laminin pathways is correlated with neuron-to-pathway adhesivity. *Dev. Biol.* 126:29–39.

Hill, T. L., and M. W. Kirschner. 1982. Subunit treadmilling of microtubules or actin in the presence of cellular barriers: possible conversion of chemical free energy into mechanical work. *Proc. Natl. Acad. Sci. USA.* 79:490–494.

Howard, T. H., and C. O. Oresajo. 1985. The kinetics of chemotactic peptide-induced change in F-actin content, F-actin distribution, and the shape of neutrophils. *J. Cell Biol.* 101:1078–1085.

Ivins, J. K., J. A. Raper, and R. N. Pittman. 1991. Intracellular calcium levels do not change during contact-mediated collapse of chick DRG growth cone structure. *J. Neurosci.* 11(6):1597–1608.

Keith, H. C. 1990. Neurite elongation is blocked if microtubule polymerization is inhibited in PC12 cells. *Cell Motil. Cytoskeleton.* 17:95–105.

Kumar, N., and M. Flavin. 1981. Preferential action of a brain detyrosinolated carboxypeptidase on polymerized tubulin. *J. Biol. Chem.* 256:7678–7686.

Lankford, K. L., and P. C. Letourneau. 1989. Evidence that calcium may control neurite outgrowth by regulating the stability of actin filaments. *J. Cell Biol.* 109:1229–1243.

Letourneau, P. C., and A. H. Ressler. 1983. Differences in the organization of actin in the growth cones compared with the neurites of cultured neurons from chick embryos. *J. Cell Biol.* 97:963–973.

Letourneau, P. C., and A. H. Ressler. 1984. Inhibition of neurite initiation and growth by taxol. *J. Cell Biol.* 98:1355–1362.

Letourneau, P. C., T. A. Shattuck, and A. H. Ressler. 1987. "pull" and "push" in neurite elongation: observations on the effects of different concentrations of cytochalasin B and taxol. *Cell Motil. Cytoskeleton.* 8:193–209.

Lim, S. S., P. J. Simak, and G. G. Borisy. 1989. Progressive and spatially differentiated stability of microtubules in developing neuronal cells. *J. Cell Biol.* 109(1):253–263.

Lumsden, A. G. S., and A. M. Davies. 1983. Earliest sensory nerve fibers are guided to peripheral targets by attractants other than nerve growth factor. *Nature (Lond.).* 396:786–788.

Mansfield, S. G., and P. R. Gordon-Weeks. 1991. Dynamic post-translational modification of tubulin in rat cerebral cortical neurons extending neurites in culture: effects of taxol. *J. Neurocytol.* 20(8):654–666.

Marsh, L., and P. C. Letourneau. 1984. Growth of neurites without filopodial or lamellipodial activity in the presence of cytochalasin B. *J. Cell Biol.* 99:2041–2047.

Okabe, S, and N. Hirokawa. 1991. Actin dynamics in growth cones. *J. Neurosci.* 11(7):1918–1929.

Omann, G. M., A. A. Rodger, G. M. Bokoch, R. G. Painter, A. E. Traynor, and L. A. Sklar. 1987. Signal transduction and cytoskeletal activation in the neutrophil. *Physiol. Rev.* 67:285–322.

Raper, J. A., and J. Kapfhammer. 1990. The enrichment of a neuronal growth cone collapsing activity from embryonic chick brain. *Neuron.* 2:21–29.

Robson, S. J., and R. D. Burgoyne. 1989. Differential localization of tyrosinated, detyrosinated, and acetylated α-tubulins in neurites and growth cones of dorsal root ganglion neurons. *Cell Motil. Cytoskeleton.* 12:273–282.

Sabry, J. H., T. P. O'Connor, L. Evans, A. Toroian-Raymond, M. Kirschner, and D. Bentley. 1991. Microtubule behavior during guidance of pioneer growth cones in situ. *J. Cell Biol.* 115(2):381–395.

Sampath, P., and T. D. Pollard. 1991. Effects of cytochalasin, phalloidin, and pH on the elongation of actin filaments. *Biochemistry.* 30:1973–1980.

Schiff, P.B., J. Fant, and S. B. Horwitz. 1979. Promotion of microtubule assembly *in vitro* by taxol. *Nature (Lond.).* 277:665–667.

Seeds, N. W., A. G. Gilman, T. Amano, M. W. Nirenberg. 1970. Regulation of axon formation by clonal lines of a neural tumor. *Proc. Natl. Acad. Sci. USA.* 66:160–167.

Shaw, G., M. Osborn, and K. Weber. 1981. Arrangement of neurofilaments, microtubules and microfilament-associated proteins in cultured dorsal root ganglion cells. *Eur. J. Cell Biol.* 24:20–27.

Smith, S. J. 1988. Neuronal cytomechanics: the actin-based motility of growth cones. *Science (Wash. DC).* 242(4879):708–715.

Spooner, B. S., and C. R. Holladay. 1981. Distribution of tubulin and actin in neurites and growth cones of differentiating nerve cells. *Cell Motility.* 1:167–178.

Stossel, T. P. 1989. From signal to pseudopod. *J. Biol. Chem.* 264(31):18261–18264.

Symons, M. H., and T. J. Mitchison. 1991. Control of actin polymerization in live and permeabilized fibroblasts. *J. Cell Biol.* 114(3):503–513.

Tanaka, E. M., and M. W. Kirschner. 1991. Microtubule behavior in the growth cones of living neurons during axon elongation. *J. Cell Biol.* 115(2):345–363.

Theriot, J. A., and T. J. Mitchison. 1991. Actin microfilament dynamics in locomoting cells. *Nature (Lond.).* 352:126–131.

Theriot, J. A., T. J. Mitchison, L. G. Tilney, and D. A. Portnoy. 1992. The rate of actin-based motility of intracellular *Listeria monocytogenes* equals the rate of actin polymerization. *Nature (Lond.).* 357:257–260.

Thompson, W. C. 1982. The cyclic tyrosination/detyrosination of alpha tubulin. *Methods Cell Biol.* 24:235–255.

Tsao, M. C., B. J. Walthall, and R. G. Ham. 1982. Clonal growth of normal human epidermal keratinocytes in a defined medium. *J. Cell. Physiol.* 110:219–229.

Wang, Y. L. 1985. Exchange of actin subunits at the leading edge of living fibroblasts: possible role of treadmilling. *J. Cell Biol.* 101:597–602.

Yamada, K. M., B. S. Spooner, and N. K. Wessells. 1970. Axon growth: roles of microfilaments and microtubules. *Proc. Natl. Acad. Sci. USA.* 66(4): 1206–1212.